論文 / 著書情報
Article / Book Information

Title	High-resolution three-dimensional holographic display using dense ray sampling from integral imaging
Authors	Koki Wakunami, Masahiro Yamaguchi, Bahram Javidi
Citation	Optics Letters, Vol. 37, No. 24, pp. 5103-5105
Pub. date	2012, 12
Copyright	Copyright (c) 2012 Optical Society of America

High-resolution three-dimensional holographic display using dense ray sampling from integral imaging

Koki Wakunami,[1,*] Masahiro Yamaguchi,[1] and Bahram Javidi[2]

[1]*Global Scientific Information and Computing Center, Tokyo Institute of Technology, 4259-R2-56 Nagatsuta, Midori-ku, Yokohama, Kanagawa 226-8503, Japan*

[2]*Electrical and Computer Engineering Dept, University of Connecticut, U-2157, Storrs, Connecticut 06269-2157, USA*

**Corresponding author: wakunami.k.aa@m.titech.ac.jp*

Received September 21, 2012; accepted October 9, 2012;
posted October 31, 2012 (Doc. ID 176412); published December 7, 2012

We present a high-resolution three-dimensional (3D) holographic display using a set of elemental images obtained by passive sensing integral imaging (II). Hologram calculations using a high-density ray-sampling plane are achieved from the elemental images captured by II. In II display, ray sampling by lenslet array and light diffraction limits the achievable resolution. Our approach can improve the resolution since target objects are captured in focus and then light-ray information is interpolated and resampled with higher density on ray-sampling plane located near the object to be converted into the wavefront. Numerical experimental results show that the 3D scene, composed of plural objects at different depths from the display, can be reconstructed with order of magnitude higher resolution by the proposed technique. © 2012 Optical Society of America

OCIS codes: 090.0090, 090.1760, 090.2870, 100.6890, 110.4190, 110.6880.

Integral imaging (II) is a three-dimensional (3D) imaging technique that uses a lenslet array to sample and reconstruct the light rays coming from an object [1]. In the pickup process, the intensity and direction of the rays that pass through a lenslet array are captured as a set of elemental images by an image sensor. Reconstruction is a reverse of the pickup process and the 3D information is visualized with full parallax. However, due to the influence of ray sampling by the lenslet array and diffraction at the lenslet aperture, there is a trade-off between the spatial resolution and depth of field [2–4].

Holography can reproduce high-resolution 3D images free from the aforementioned limitations by using coherent light. For an electronic display of holography, a digitized interference pattern is required, and can be obtained through digital holography from a real object or scene. An interference pattern can also be calculated from virtual 3D data, known as computer-generated hologram (CGH). Recently, Mishina and Okano proposed a CGH calculation method from the elemental images captured by II technique for a real scene [5]. In his technique, reconstructed wavefront by II display is simulated numerically and recorded on the CGH plane; therefore, image resolution is identical with the II display case.

Recently, we proposed a CGH calculation method using a virtual ray-sampling (RS) plane located near the object, as shown in Fig. 1 [6]. On the RS plane, the rays from the object are sampled in high density spatially and angularly. Ray information of each sample point corresponds to the projection image and can be obtained by using general rendering software from 3D data in computer. Complex amplitude distribution around each RS point is derived by applying Fourier transform for each projection image based on the angular spectrum theory. This process is considered as the conversion from ray information into the wavefront. Then, wave propagation from RS plane to CGH plane is calculated to obtain the wavefront on the hologram. In [5], we optically demonstrated image reconstruction for only the virtual object.

In this Letter, we show a new application of our CGH computation method for a real scene with II sensing. To reconstruct a high-resolution image for a deep 3D scene, plural objects located at different depths are captured in focus. Then, light rays captured as elemental images are interpolated and converted into wavefronts on the RS plane set near each object. The hologram pattern is obtained by synthesizing the wavefronts from those objects. This approach can overcome the resolution of general II display or II-based holographic displays.

In II display, there are two types of reconstruction [4]. One is resolution priority II (RPII) where the distance between the lenslet array and an imaging device should be larger than the focal length of the lenslet to focus on the object. Another one is depth priority II (DPII) where an imaging device is located at the focal plane of the lenslet.

In practical cases, since a discretized imaging device is used, rays are sampled angularly and the reconstructed image has a resolution limit δ_a given by

$$\delta_a = |z_{\text{object}}| \cdot \Delta\theta_a, \tag{1}$$

where z_{object} is the distance from a lenslet array to the object's surface and $\Delta\theta_a$ is the angular resolution of sampled rays. Even if the rays are sampled with high density to achieve small $\Delta\theta_a$, image resolution is still limited by light diffraction. In RPII case, each lenslet behaves as an imaging lens and the light is focused on the lens image plane (LIP). In this case, the resolution limit $\delta_{d\text{–RPII}}$ [Fig. 2(a)] is approximately given by

$$\delta_{d\text{–RPII}} = \frac{\lambda |z_{\text{LIP}}|}{d}, \tag{2}$$

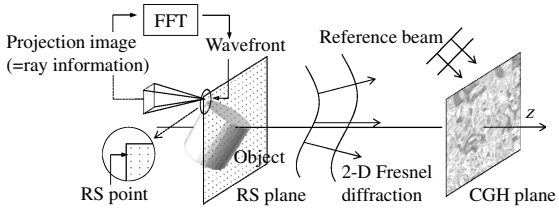

Fig. 1. CGH calculation model using ray-sampling (RS) plane.

0146-9592/12/245103-03$15.00/0

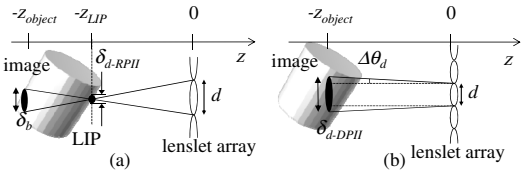

Fig. 2. Resolution factors by light diffraction. (a) RPII and (b) DPII.

where λ is the wavelength of the light. In addition, due to divergence of the light from LIP, resolution limit δ_b for an out-of-focus image is proportional to the image distance from LIP [see Fig. 2(a)] as

$$\delta_b = \frac{d|z_{\text{object}} - z_{\text{LIP}}|}{|z_{\text{LIP}}|}. \tag{3}$$

According to Eqs. (2) and (3), due to trade-off by lenslet size d, it is not possible to reconstruct higher-resolution images for deep 3D scenes. In DPII case, each lenslet behaves like a collimating lens. Reconstructed rays should be plane waves with diffracted beams broadening, as shown in Fig. 2(b). The ray broadening angle $\Delta\theta_d$ is $\sin^{-1}(\lambda/(2d))$. The resolution limit $\delta_{d-\text{DPII}}$ on the image is given by

$$\delta_{d-\text{DPII}} = d + \frac{\lambda|z_{\text{object}}|}{d}. \tag{4}$$

DPII system with larger lenslets is better for degradation due to light diffraction for deep 3D scene. However, resolution limit $\delta_{d-\text{DPII}}$ cannot be less than lenslet size. Even if d is decreased, the light diffraction will increase and the depth priority will suffer. The limitations of ray sampling and light diffraction make it difficult to reproduce an image with higher resolution for deep 3D scene by conventional II and II-based holographic displays.

The proposed approach is executed through the following procedure. Initially, a set of elemental images is obtained as input images by a synthetic aperture II (SAII) system [7] in RPII mode. In the case of a target scene that consists of plural objects located at different depths, each object is captured in focus respectively. Then, ray information on the RS planes are resampled as projection images from input images by using image-based rendering (IBR) technique [see Fig. 3(a)]. Several IBR techniques have been proposed by geometric model, depth information, and feature matching, and the proper one should be selected with consideration for the parameter of input images and target scene. Light field rendering (LFR) is one kind of IBR technique that permits the rendering of a free-viewpoint image from a set of multi-view images by simply using a single plane, called focal plane, to approximate the object space [8]. Since each object is assumed to have narrow depth range in this Letter, LFR

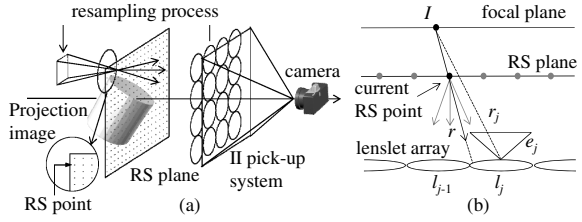

Fig. 3. Light ray resampling. (a) II pick up and (b) LFR process.

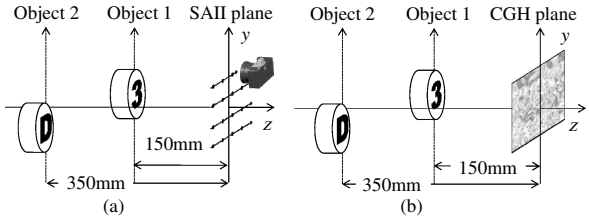

Fig. 4. (a) Pickup scene by SAII. (b) Scheme of holographic display.

by a single focal plane is applied for the resampling process. If the objects have wide depth ranges, layered focal planes to synthesize free blurring artifacts from approximation proposed by Isaksen *et al.* can be applied [9].

Figure 3(b) shows a configuration of ray resampling process by LFR. l_j and e_j denote the jth lenslet and elemental image, respectively. Focal plane is referred to the nearby object, and thus is located on the LIP of RPII pickup system. The RS plane is located near the focal plane. Now, a desired ray's intensity r, which intersects current RS point and the focal plane at I, will be obtained from the intensity of r_j. r_j intersects I and l_j that r passes through the lenslet array. This is the simplest LFR model. Note that the unsampled ray by pickup system such as r is interpolated on the condition that the focal plane (i.e., the object approximated plane) emits equivalent intensity between the desired ray and closest sampled ray. The projection image can be obtained by repeating this process for each ray on the RS point. Projection images obtained by resampling process are multiplied by random phase distribution to equalize the power spectrum on the RS plane, and then are transformed into the complex amplitude distribution by using fast Fourier transform. By tiling the complex amplitude distribution of each projection image, the whole two-dimensional (2D) wavefront on the RS plane is obtained. Light propagation from the RS plane to CGH plane is calculated by 2D Fresnel diffraction. Finally, the interference pattern between the wavefront from the RS plane and reference beam is calculated.

Reconstructed image resolution by our approach should be estimated from three factors: resolution limitation by pickup process, degradation by ray sampling, and light diffraction on the RS plane.

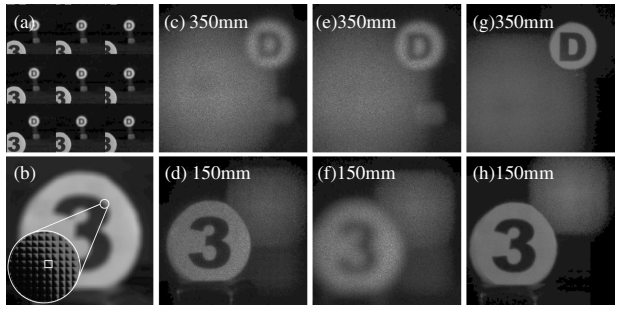

Fig. 5. (a) Subset of elemental images focusing on object1 (see Fig. 4), (b) resampled rays on the RS plane of object1 (a white square illustrates a projection image of a RS point), (c)–(h) reconstructed images by numerical simulation (top row focusing on object 2 and bottom row focusing on object 1), (c), (d) results by RPII-based CGH, (e), (f) results by DPII-based CGH, and (g), (h) results by proposed approach.

Table 1. Estimated Image Resolutions by Each Approach

	RPII-Based CGH		DPII-Based CGH		Proposed CGH	
Resolution Factor	Object 1	Object 2	Object 1	Object 2	Object 1	Object 2
δ_a by Eq. (1)	0.075	0.17	0.075	0.17	0.075(0.02)	0.17(0.02)
$\delta_{d-\mathrm{RPII}}$ or (δ_b) by Eqs. (2) and (3)	0.053	(2.0)	—	—	0.053	0.12
$\delta_{d-\mathrm{DPII}}$ by Eq. (4)	—	—	1.55	1.62	0.10	0.10

Because each object located at different depth is captured in focus, high resolution images are obtained in the pickup process. To avoid multiple capturing for plural objects, one-shot capturing with filtering tool to extend the depth of field can be also applied for the pickup process [10]. The resolution limitation by ray sampling and light diffraction on an RS plane can be estimated using Eqs. (1) and (4) since each RS point behaves like a lenslet of DPII. Here, d and z_{object} in these equations correspond to the pitch of RS points and distance between the RS plane and the object, respectively. Since an RS plane is set near each object and rays are sampled with high density (i.e., d and z_{object} are much smaller than conventional DPII case), those degradation factors can also be suppressed for even a deep 3D scene with plural objects.

We performed numerical simulation to confirm that the proposed approach can overcome the limitation of conventional II-based holographic display. Reconstructed images by the proposed approach are compared with the conventional CGHs based on RPII and DPII displays.

In the pickup process, 16×16 elemental images in 256×256 pixels each ($\Delta\theta_a = 0.029$ deg) were captured by a SAII system [7]. Two objects were located at 150 and 350 mm from SAII [Fig. 4(a)]. Lenslet pitch p, equal to lenslet size d, was 1.5 mm. For conventional CGHs based on RPII or DPII, elemental images were captured focusing on the object 1 (i.e., $z_{\mathrm{LIP}} = 150$ mm) or infinity to set the image sensor at focal length of camera lens as DPII sensing, respectively. For the proposed approach, both objects were captured in focus respectively.

In both conventional and proposed approaches, holographic displays were set at the SAII plane [Fig. 4(b)]. Final CGHs had 8192×8192 pixels with 2 μm pixel pitch. In conventional CGHs, the parameters of the lenslet were identical to the pickup process. Outgoing wavefronts by RPII/DPII from the lenslet array were calculated by simulating light propagation from input images and the phase modulation of lenslets then recorded as holograms. In the proposed method, RS planes were set at 5 mm in front of both objects and have 256×256 RS points with 64 μm pitch. Each point resamples 32×32 rays ($\Delta\theta_a = 0.23$ deg) as projection image by LFR [Fig. 5(b)]. After the wave propagation from the RS planes to the CGH plane, the wavefronts from both planes are superposed on the CGH plane to obtain the final wavefront.

In numerical reconstruction, an observer was set 100 mm from CGH displays and the observer's eye imaging (pupil size is 7 mm) was simulated in wave optics. Wavelength λ was 532 nm in this simulation.

The estimated resolution factors by Eqs. (1)–(4) of each approach are shown in Table 1. In the conventional CGH displays, each factor is estimated with the parameters of the pickup process, $\Delta\theta_a = 0.029$ deg, $d = 1.5$ mm, $z_{\mathrm{LIP}} = 150$ mm since LIP was set at object 1 in the RPII case. Maximum values for each object are underlined in the table as a dominant factor of resolution. Object 1 can be reconstructed with high resolution by the RPII case, but object 2 in the RPII case and both objects in the DPII case are degraded significantly.

For the proposed method, δ_a and $\delta_{d-\mathrm{RPII}}$ from the pickup process were derived with the same $\Delta\theta_a$, d, z_{object} in the RPII case, and $z_{\mathrm{LIP}} = 150$ mm/350 mm for object1/object2 in Eq. (2) since both objects were captured in focus. δ_a (in parentheses in Table 1) and $\delta_{d-\mathrm{DPII}}$ due to ray sampling and light diffraction by RS plane were derived with $z_{\mathrm{object}} = 5$ mm, $\Delta\theta_a = 0.23$ deg, $d = 64$ μm for both objects. Thus, dominant resolutions for object 1 and object 2 are estimated as 0.10 and 0.17 mm, respectively.

Reconstructed images by numerical simulation are shown in Figs. 5(c)–5(h). The proposed approach sharply reconstructs each object [Figs. 5(g) and 5(h)] for deep scene consistent with the estimated theoretical resolutions. The conventional CGH displays produce blurred images for deep scene [Figs. 5(c)–5(f)].

In conclusion, a high-resolution 3D holographic display using elemental images captured by II [1–4,11,12] is described. We demonstrated that the proposed approach may overcome the resolution limitation of the displays based on II by ray interpolation and resampling on the RS plane by IBR technique. Numerical simulation shows that the proposed method can reconstruct a 3D scene composed of plural objects located at different depths from display with higher resolution than conventional CGH display based on the II reconstruction.

References

1. G. Lippmann, C. R. Acad. Sci. Paris Ser. IV **146**, 446 (1908).
2. C. B. Burckhardt, J. Opt. Soc. Am. **58**, 71 (1968).
3. H. Hoshino, F. Okano, H. Isono, and I. Yuyama, J. Opt. Soc. Am. A **15**, 2059 (1998).
4. F. Jin, J. S. Jang, and B. Javidi, Opt. Lett. **29**, 1345 (2004).
5. T. Mishina and F. Okano, Appl. Opt. **45**, 4026 (2006).
6. K. Wakunami and M. Yamaguchi, Opt. Express **19**, 9086 (2011).
7. J. S. Jang and B. Javidi, Opt. Lett. **27**, 13 (2002).
8. M. Levoy and P. Hanrahan, in *Proceedings of the 23rd Annual Conference on Computer Graphics and Interactive Techniques (SIGGRAPH '96)* (ACM, 1996), pp. 31–42.
9. A. Isaksen, L. McMillan, and S. J. Gortler, *Proceedings of the 27th Annual Conference on Computer Graphics and Interactive Techniques (ACM SIGGRAPH '00)* (ACM, 2000), pp. 297–306.
10. R. Martinez-Cuenca, G. Saavedra, M. Martinez-Corral, and B. Javidi, J. Disp. Technol. **1**, 321 (2005).
11. R. Martinez-Cuenca, G. Saavedra, M. Martinez-Corral, and B. Javidi, Proc. IEEE **97**, 1067 (2009).
12. A. Stern and B. Javidi, Proc. IEEE **94**, 591 (2006).